Vibrational specific simulation of nonequilibrium radiation from shock-heated air

Wei Su, Domenico Bruno, and Yacine Babou

Citation: AIP Conference Proceedings **1786**, 150001 (2016); doi: 10.1063/1.4967642
View online: http://dx.doi.org/10.1063/1.4967642
View Table of Contents: http://scitation.aip.org/content/aip/proceeding/aipcp/1786?ver=pdfcov
Published by the AIP Publishing

Vibrational Specific Simulation of Nonequilibrium Radiation from Shock-Heated Air

Wei Su[1], Domenico Bruno[1,a)] and Yacine Babou[2]

[1]*Istituto di Nanotecnologia, Consiglio Nazionale delle Ricerche, 70126, Bari, Italy*
[2]*Departamento de Bioingeniería Ingeniería Aeroespacial, Universidad Carlos III de Madrid, 28911, Madrid, Spain*

[a)]Corresponding author: domenico.bruno@cnr.it

Abstract. The vibration-specific State-to-State approach is employed to described vibrational relaxation and reactive processes in shock-heated air. The gas mixture consists of the five chemical species N_2, O_2, NO, N and O. Making use of two different sets of quasi-classical trajectory calculations for the Zeldovich exchange reactions of NO formation on theoretically calculated potential energy surfaces, the thermal and chemical kinetics of NO is discussed in detail. Then the emission spectra are determined and compared to shock tube measurements.

INTRODUCTION

During the re-entry of a spacecraft into a planetary atmosphere, the relative stream velocity is so high that a bow shock is created in front of the vehicle. After the strong shock wave, in the relaxing flow, a massive amount of the free stream kinetic energy is converted through inelastic collisions, into internal energy of the surrounding gases, which results in intense convective and radiative heating over the spacecraft structure. Inter-particle collisions promote energy exchanges among the internal modes of atoms and molecules, and produce chemical reactions including dissociation and ionization. Since the time scale of energy exchange processes for internal levels and the chemical time scale is comparable with the aerodynamics one, the flow behind the shock is in thermal and chemical nonequilibrium. Understanding such nonequilibrium processes in shock-heated flows is a key issue for the design of the spacecraft. Although progress has been achieved during the last decades, modeling of thermo-chemically nonequilibrium flows is still a challenging problem in both academia and industry.

The state of the gas, i.e. the concentration of the gas species and their internal energy (rotational, vibrational and electronic) level populations can be estimated by either multi-temperature (MT) models [1] or state-to-state (StS) approaches [2]. The MT models make the assumption that each energy mode is characterized by its own temperature, which is determined by solving an individual energy conservation equation. These models rely on the common assumption that the relaxation of the internal energy modes occurs through a series of Boltzmann distributions at their respective temperatures. However, in many flow conditions, the populations deviate from Boltzmann distributions [1]. Conversely, the StS approaches treat each molecule with different internal state as a separate pseudo-species, for which a continuity equation is solved. Without adopting any quasi-stationary distribution over the internal energy modes, these approaches allow representing arbitrary nonequilibrium situations.

The StS approaches however, require a large number of reaction rate constants corresponding to the different physico-chemical processes. The most advanced models take into account the full set of rotational, vibrational and electronic transitions, as well as radiative processes for atomic and molecular species [3, 4, 5]. Due to the lack of knowledge of all the required reaction rates, these models were restricted to pure nitrogen or pure oxygen flows. In this study, the nonequilibrium relaxation in shock-heated air is simulated with a StS approach, since the vibrational state-specific rate coefficients from *ab initio* methods are becoming available to describe vibrational relaxation and reactive processes in N_2-O_2 mixtures. Particularly sensitive is the population of NO whose formation is governed by a strong coupling between chemical and vibrational kinetics. NO being a strong radiator, accurate prediction of the NO formation dynamics is crucial to the correct understanding of the flow radiation signature. Making use of recent quasi-classical trajectory (QCT) results for the Zeldovich exchange reactions of NO formation on theoretically

30th International Symposium on Rarefied Gas Dynamics
AIP Conf. Proc. 1786, 150001-1–150001-8; doi: 10.1063/1.4967642
Published by AIP Publishing. 978-0-7354-1448-8/$30.00

calculated potential energy surfaces (PES), the thermal and chemical kinetics of NO is discussed in detail. Then, the radiative signature is determined on the basis of the spectroscopic database HTGR [6] tabulating exhaustive radiative properties validated at high temperature for NO and N_2 radiative systems. Simulated spectra are compared to shock tube measurements performed in Moscow [7] in conditions representative of Earth re-entries ($u \sim 4-8$ km/s).

MODELLING

In the present work, we consider an air gas mixture consisting of the five chemical species N_2, O_2, NO, N and O. For the shock conditions of interest, the ionization degree is expected to be small and the focus is on the coupling of vibrational and chemical kinetics. Thereby, ionization is neglected and all the species are assumed to be on the ground electronic state. A vibrational state-specific description is adopted for the molecular species N_2, O_2 and NO. Vibrational levels are obtained from a RKR analysis on the low energy part of spectroscopically determined potential energy curves and the extrapolation to the dissociation limit[8]. This gives a total of 61 bound levels for N_2, 46 for O_2 and 48 for NO. Rotational mode is assumed in equilibrium at the gas temperature T. In the following paragraphs, the physical model applied for the simulation of shock tube flows is presented.

Governing Equations

In the frame of reference moving with the shock, the flow is conveniently described by the stationary 1D Euler equations for the $n = 157$ chemical species:

$$\partial_x (\rho u) = 0 \tag{1}$$

$$\partial_x \left(\rho u y_k^v\right) = \dot{\omega}_k^v, \quad v = 0...v_{\max}^k,\ k \in \mathbb{H} \tag{2}$$

$$\partial_x \left(\rho u^2 + p\right) = 0 \tag{3}$$

$$\partial_x \left[\rho u \left(h + \frac{u^2}{2}\right)\right] = 0 \tag{4}$$

with $\mathbb{H} = \{N_2, O_2, NO, N, O\}$. ρ, u, p and h are the density, velocity, total pressure and specific enthalpy of the gas mixture, respectively. y_k^v and $\dot{\omega}_k^v$ are the mass fraction and source term of the molecular species k with vibration level v. $v_{\max}^k$ is the maximum vibrational quantum number for species k and $v_{\max}^k = 0$ for atoms. Then, the species mass fractions and related chemical source terms are obtained by summing over all vibrational levels, i.e. $y_k = \sum_{v=0}^{v_{\max}} y_k^v$, $\dot{\omega}_k = \sum_{v=0}^{v_{\max}} \dot{\omega}_k^v$. The conservation equations are completed by closure relations obtained from the ideal gas assumption and then solved by the ODEPACK library [9].

Vibration-Chemical Kinetic Mechanism and the Reaction Rates

Three categories of physico-chemical processes are included in this work: 1) vibration-translation (VT) energy exchange: $AB(v) + M \rightleftharpoons AB(w) + M$; 2) dissociation-recombination (DR): $AB(v) + M \rightleftharpoons A + B + M$; 3) Zeldovich exchange (ZE): $AB(v) + C \rightleftharpoons AC(w) + B$. Denoting by $s_r^{k,i}$ and $s_p^{k,i}$ the reactant and product stoichiometric coefficients of species k in reaction i, the state-specific chemical source term $\dot{\omega}_{k,v}^i$ is expressed as:

$$\dot{\omega}_{k,v}^i = M_k \cdot \left(s_p^{k,i} - s_r^{k,i}\right) \cdot \left(k_f^i \cdot \prod_{k=1}^{n} [N_{k,v}]^{s_p^{k,i}} - k_b^i \cdot \prod_{k=1}^{n} [N_{k,v}]^{s_r^{k,i}}\right) \tag{5}$$

where $[\cdot]$ denotes molar density. k_f^i and k_b^i are respectively the forward and backward reaction rate constants. They satisfy the detailed balance condition $k_b^i = k_f^i / k_{\text{eq}}^i$, k_{eq}^i being the equilibrium constant. Then the chemical source term $\dot{\omega}_{k,v}$ is the sum of the source $\dot{\omega}_{k,v}^i$ over all the processes, $\dot{\omega}_{k,v} = \sum_i \dot{\omega}_{k,v}^i$.

Values for the state-specific rates are obtained, where available, from quasi-classical trajectory (QCT) calculations on *ab inito* potential energy surfaces. Alternatively, rate coefficients are calculated from the semi-analytical Forced Harmonic Oscillator (FHO) model. For the remaining processes, where none of the above is available, the classical models of Landau-Teller (LT) relaxation (for VT) and Park's two temperature model (for DR) are used.

Table 1. Vibration-chemical kinetic mechanism

Reaction	Model	Reaction	Model
$N_2(v) + N_2 \rightleftharpoons N_2(w) + N_2$	FHO	$N_2(v) + N \rightleftharpoons 3\,N$	QCT
$N_2(v) + O_2 \rightleftharpoons N_2(w) + O_2$	FHO	$N_2(v) + O \rightleftharpoons 2\,N + O$	QCT
$N_2(v) + N \rightleftharpoons N_2(w) + N$	QCT	$N_2(v) + NO \rightleftharpoons 2\,N + NO$	Park
$N_2(v) + M \rightleftharpoons N_2(v) + M$ $M \in \{NO, O\}$	LT	$O_2(v) + N_2 \rightleftharpoons 2\,O + N_2$	FHO
$O_2(v) + N_2 \rightleftharpoons O_2(w) + N_2$	FHO	$O_2(v) + O_2 \rightleftharpoons 2\,O + O_2$	FHO
$O_2(v) + O_2 \rightleftharpoons O_2(w) + O_2$	FHO	$O_2(v) + O \rightleftharpoons 3\,O$	QCT
$O_2(v) + O \rightleftharpoons O_2(w) + O$	QCT	$O_2(v) + N \rightleftharpoons 2\,O + N$	QCT
$O_2(v) + M \rightleftharpoons O_2(v) + M$ $M \in \{NO, N\}$	LT	$O_2(v) + NO \rightleftharpoons 2\,O + NO$	Park
$NO(v) + N_2 \rightleftharpoons NO(w) + N_2$	FHO	$NO(v) + N_2 \rightleftharpoons N + O + N_2$	FHO
$NO(v) + O_2 \rightleftharpoons NO(w) + O_2$	FHO	$NO(v) + O_2 \rightleftharpoons N + O + O_2$	FHO
$NO(v) + M \rightleftharpoons NO(v) + M$ $M \in \{NO, N, O\}$	LT	$NO(v) + M \rightleftharpoons N + O + M$ $M \in \{NO, N, O\}$	Park
$N_2(v) + N_2 \rightleftharpoons 2\,N + N_2$	FHO	$N_2(v) + O \rightleftharpoons NO(w) + N$	QCT
$N_2(v) + O_2 \rightleftharpoons 2\,N + O_2$	FHO	$O_2(v) + N \rightleftharpoons NO(w) + O$	QCT

Table 1 summarizes the state-specific reactions used in this work and the methods used to calculate the reaction rate constants.

State-Specific Rates From Classical Models

The LT model assumes vibrational energy relaxes as a consequence of VT energy transfer collisions as:

$$\Omega^*_{\mathrm{VT}} = \rho_{AB} \frac{e^{AB}_{\mathrm{vib,eq}}(T) - e_{AB,\mathrm{vib}}}{\tau_{AB-M}} \tag{6}$$

where $e^{AB}_{\mathrm{vib,eq}}(T)$ is the specific vibrational energy in equilibrium at temperature T; τ_{AB-M} is the relaxation time and is modelled from the Millikan-White's formula [10]. In a StS framework, this behaviour is recovered by choosing the state-specific rates as:

$$k_f^{v\to w} = \frac{1}{N_A[M]} \cdot \left(\frac{y^w_{AB}}{y_{AB}}\right)_{\mathrm{eq}} \cdot \frac{1}{\tau_{AB-M}}, \quad k_b^{v\to w} = k_f^{w\to v} \tag{7}$$

where N_A is Avogadro's number and $\left(\frac{y^w_{AB}}{y_{AB}}\right)_{\mathrm{eq}}$ is the equilibrium population. Backward rates are calculated from the detailed balance condition, with $k_{eq}^{v\to w} = \exp\left(-\frac{\epsilon^w_{AB} - \epsilon^v_{AB}}{k_B T}\right)$.

Next, the Park's two temperature model [1] for a dissociation/recombination reaction, $AB + M \rightleftharpoons A + B + M$, assumes the rate coefficients can be expressed by modified Arrhenius functions:

$$K_f(T_f) = \alpha \cdot T_f^{\beta} \cdot \exp\left(-\frac{\gamma}{T_f}\right), \quad K_b(T_b) = \frac{K_f(T_b)}{K_{\mathrm{eq}}(T_b)} \tag{8}$$

where the constants α, β, γ are adjusted to reproduce experimental determinations of K_f and K_{eq}. T_f and T_b are the effective temperatures for the direct and inverse reactions, respectively and are chosen as $T_f = \sqrt{T \cdot T^{\mathrm{vib}}_{AB}}$, $T_b = T$. The energy-representative vibrational temperature T^{vib}_{AB} is the temperature for which a Boltzmann distribution would give the same vibrational energy as the non-equilibrium distribution. Then, the chemical and vibrational energy source terms are obtained by:

$$\dot{\omega}^*_{AB} = -M_{AB} N_A \left(K_f[AB][M] - K_b[A][B][M]\right) \tag{9}$$

$$\Omega^*_{\mathrm{DR}} = -M_{AB} N_A \left(K_f[AB][M]\,\langle E_d\rangle_{AB} - K_b[A][B][M]\,\langle E_r\rangle_{AB}\right) \tag{10}$$

where $\langle E_d \rangle_{AB}$, $\langle E_r \rangle_{AB}$ are the average vibrational energy lost/gained in dissociation/recombination. In practice, it is usually set $\langle E_d \rangle = \langle E_r \rangle = e_{\text{vib}}(T^{\text{vib}})$ by assuming the reaction has a non-preferential character. In a StS approach, the above behaviour is reproduced by choosing:

$$k_f^v = K_f(T_f), \tag{11}$$

$$k_b^v = \frac{k_f^v}{k_{\text{eq}}^v}, \quad k_{\text{eq}}^v = K_{\text{eq}}(T) \frac{\sum_{v=0}^{v_{\max}} \exp\left(-\epsilon_{AB}^v / k_B T_{AB}^{\text{vib}}\right)}{\exp\left(-\epsilon_{AB}^v / k_B T_{AB}^{\text{vib}}\right)} \tag{12}$$

State-Specific Rates From FHO or QCT Calculations

The rates for vibrational excitation and dissociation in diatom-diatom collisions are taken from the STELLAR Database [11]; it collects results from the work of Lino da Silva *et al.*, who applied the FHO model [12] to the production of a multiquantum datasets of VT and DR rates [13] in a wide temperature range. The excitation and dissociation rates for N_2-N and O_2-O systems are from the work of Esposito *et al.* based on the QCT approach [14, 15]. For the two Zeldovich exchange reactions, we use two alternative datasets: one from Bose and Candler [16, 17] and one from the very recent work by Esposito [18]. The dissociation rates in N_2-O and O_2-N collisions are also from this recent work. Note that all datasets have been adapted to the vibrational levels specified above by a linear fitting on the vibrational energy. In addition, a unique set of equilibrium constants [7] is employed throughout.

Radiative Signature Modelling

In the following we present the approach adopted to rebuild the radiative signature measured in the frame of shock tube experiments. We restrict our interest to the case 8.06 km/s for which the radiative signature is documented in the UV spectral range in absolute units. The radiative signature is computed by means of the high resolution spectroscopic databases HTGR [6]. The electronic systems of radiative transitions that have been considered for the computation are N_2 Second-Positive ($C^3\Pi_u - B^3\Pi_g$), O_2 Schumann-Runge ($B^3\Sigma_u^- - X^3\Sigma_g^-$) and NO γ ($A^2\Sigma^+ - X^2\Pi_r$), β ($B^2\Pi_r - X^2\Pi_r$, δ ($C^2\Pi_r - X^2\Pi_r$) and 10000 Angstrom ($D^2\Sigma^+ - A^2\Sigma^+$).

For a radiative transition between an upper energy level u and a lower energy level l, the associated emission and absorption coefficients, respectively η_σ and κ_σ are calculated as:

$$\eta_\sigma = \sum_{ul} n_u \frac{A_{ul}}{4\pi} hc\sigma_{ul} f(\sigma - \sigma_{ul}), \quad \kappa_\sigma = \sum_{ul} (n_l B_{lu} - n_u B_{ul}) h\sigma_{ul} f(\sigma - \sigma_{ul}) \tag{13}$$

where n_u, resp. n_l is the population of the upper level, resp. the lower level, A_{ul}, B_{ul} and B_{lu} are the Einstein coefficients respectively for emission, induced emission and absorption processes, σ_{ul} is the wavenumber of the transition, h is the Planck constant, c is the light velocity and $f(\sigma - \sigma_{ul})$ is the line profile shape approximated by a Doppler profile to account for the thermal broadening.

For well defined energy level of a diatomic molecule (n, v, J), characterized by the electronic state n and the vibrational, resp. rotational, quantum number v, resp. J, the different contribution to the energy is separated as follows:

$$E(n, v, J) = E_{el}(n) + E_{vib}(n, v) + E_{rot}(n, J) + E_{inter}(n, v, J) \tag{14}$$

where E_{el}, $E_{vib}(n, v)$ and $E_{rot}(n, J)$ are respectively the pure electronic, vibrational and rotational term and $E_{inter}(n, v, J)$ is the vibrational-rotational interaction term (in practice much smaller than the other the terms). In the frame of the two temperatures assumption, the population of a given energy level is written as :

$$n_{nvJ} = N \frac{g_{nvJ}}{Q(T_{ve}, T_{rot})} \exp\left(-\frac{E_{el}(n) + E_{vib}(n, v)}{k_B T_{ve}}\right) \exp\left(-\frac{E_{rot}(n, J) + E_{inter}(n, v, J)}{k_B T_{rot}}\right) \tag{15}$$

where $Q(T_{ve}, T_{rot})$ is the two temperatures partition function, N is the total population of the considered molecule and g_{nvJ} is the degeneracy of the level (n, v, J). Population density N and temperatures T_{ve} and T_{rot} are taken from the previous sections.

In measurements, the intensity emitted by the flow in direction perpendicular to the its axis was collected by means of Optical Emission Spectroscopy technique corresponding to the local emission integrated first along the flow

diameter and then along the axis. Uniform properties are assumed in the radial direction. The so-called collected intensity is therefore calculated as:

$$I_\sigma^{coll} = \frac{1}{\Delta x}\int_{\Delta x} I_\sigma(x)dx, \quad I_\sigma(x) = \frac{\eta_\sigma(x)}{\kappa_\sigma(x)}(1 - e^{-\kappa_\sigma(x)D}) \tag{16}$$

where $I_\sigma(x)$ is the intensity for a given location x. The shock diameter D is assumed to be equal to the shock-tube test section diameter 5 cm and $\eta_\lambda(x)$ and $\kappa_\lambda(x)$ are the emission and absorption coefficients at the location x (along the flow axis). $\Delta x = v_{shock} \times t_{rad}$ is the length of the flow axial extent, and $t_{rad} = 6\,\mu$s refers to the effective duration of the radiation when passing through the measurement test section. Finally, for proper comparisons with measured spectra, the collected intensity is convoluted with a normalized Gaussian function of 2 nm width to account for the apparatus function broadening.

RESULTS AND DISCUSSIONS

We consider a shock wave propagating at $u = 8.06\,$km/s in a mixture of N_2 and O_2 (80%/20% molar fraction composition) at $T_1 = 298\,$K, $p_0 = 0.25\,$Torr. The conditions just behind the shock are obtained assuming frozen chemistry and vibrational kinetics. The detailed State-to-State approach is used to solve for the evolution of the flow behind the shock wave. We employed two different models of state-specific rates for the Zeldovich exchange reactions, i.e. Esposito's and Bose's rates, which are labeled as 'Espo' and 'Bose' in the following figures respectively.

Figure 1 shows the profiles of the gas and vibrational temperatures (left panel) and species mole fractions (right panel) up to 1 m behind the shock. The solid lines are the results obtained with Esposito's ZE rates, and dashed lines are those obtained from Bose's ZE rates. Differences are only noticeable for the vibrational temperature and abundance of NO. At the shock, the gas temperature increases rapidly and reaches about 31500 K. After the shock, the vibrational temperatures of N_2 and O_2 increase up to a maximum due to VT transitions. Then, once sufficient dissociation occurs, the loss of vibrational energy by dissociation takes over the energy gain due to excitation, the two temperatures fall and gradually equilibrate with the gas temperature.

The two models for the ZE reactions result in large differences in the predicted evolution of the NO vibrational temperature.

The composition profiles show the dissociation of N_2 and O_2 and the formation of NO, N and O. At the early phase of the relaxation, the low vibrational temperatures of N_2 and O_2 prevent the dissociation and exchange processes to occur. Therefore, their mole fractions remain at the initial levels before 1×10^{-5} m. Then, due to VT excitation, the molecules gradually climb the vibrational ladder, which initializes the dissociation of upper levels. As the vibrational temperatures increase, the dissociation progressively goes deep into the lower energy levels. As a result, the molecules N_2 and O_2 are dramatically reduced, while the atoms N and O are abundantly produced. At about 1×10^{-1} m, the mole fraction of N_2 is reduced from 80% to 10%. Dissociation of O_2 is faster so that already at 1×10^{-3} m, the mole fraction of O_2 falls to below 0.1%. NO, instead, is produced in the Zeldovich exchange reactions. The onset of these processes requires enough atomic nitrogen and oxygen from dissociation of N_2 and O_2. Therefore, a long incubation distance is observed for the appearance of NO. Esposito's rates predict a relatively larger formation than Bose's rates. At about 2×10^{-5} m, Esposito's rates predict more than 0.1% mole fraction of NO, which reaches its maximum value of 0.65% at 8×10^{-5} m. Bose's rates obtain more than 0.1% NO at 4×10^{-5} m, and then get the maximum value of 0.24% at 1.7×10^{-4} m. After the peak, dissociation prevails over formation, and the mole fraction of NO begins to curve. At 1×10^{-3} m, the mole fraction of NO falls back below 0.1%.

In order to explain the observed behaviour, profiles of vibrational energy source terms pertaining to the different processes are plotted in Figure 2. These are defined as:

$$\Omega_i = \sum_{v=0}^{v_{\max}} \dot{\omega}^i_{AB(v)} \epsilon^v_{AB}, \quad i \in \{\mathrm{VT}, \mathrm{DR}, \mathrm{ZE}\} \tag{17}$$

We also define preferential energy source terms for DR and ZE processes as $\Omega_i^{\mathrm{Pref}} = \Omega_i - \dot{\omega}^i_{AB} \cdot e^{AB}_{\mathrm{vib}}$, $i \in \{\mathrm{VT}, \mathrm{DR}\}$. These terms express the preferentiality of the chemistry-vibration coupling and can be directly related to the evolution of the vibrational temperatures. In Figure 2, the upper plots show the VT (red lines), DR (blue lines) and ZE (green lines) vibrational energy source terms, as well as their sum (black lines). The lower plots show the VT (red lines), preferential DR (blue lines) and preferential ZE (green lines) energy source terms, and their sum (black lines). The positivity/negativity of VT energy source term reflects the overshoot/undershoot of vibration temperature to translation

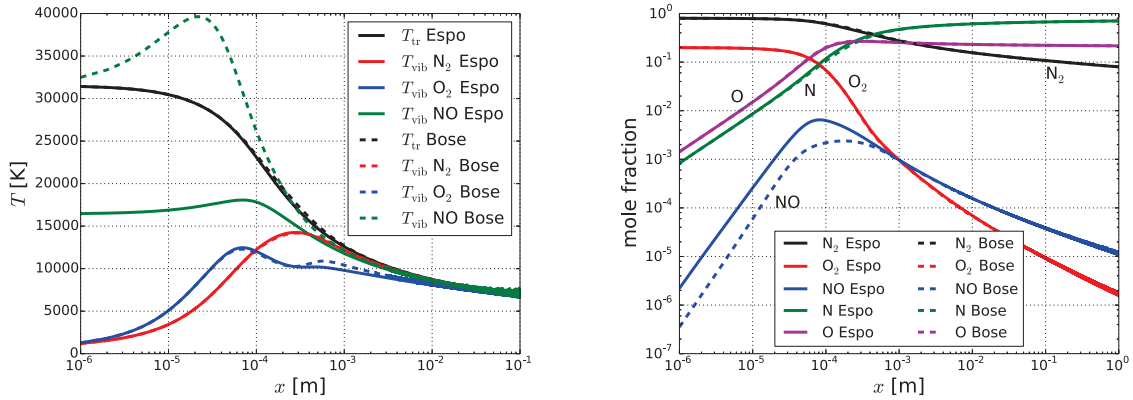

Figure 1. Profiles of the temperature and mole fractions behind the shock wave

one, while the positivity/negativity of DR or ZE energy source term reflects the gain/loss of species. Finally, the positivity/negativity of preferential energy source term describes the rise/drop of vibrational temperature.

The VT terms for N_2 and O_2 show similar behaviour, being positive and monotonically decreasing after the shock: it illustrates how the vibrational temperatures of the two species are always lower than the translational one, and they gradually relax to equilibrium. The VT source term for NO from Esposito's rates is also positive but rises first then drops, which accommodates the change in the amount of substance. On the other hand, Bose's rates predict that the NO is created at temperatures higher than the translational one; the corresponding VT source term first quickly falls to the negative minimum value and then gradually increases to positive values due to de-excitation and dissociation processes. At about 1.9×10^{-4} m, the dissociation outweighs the exchange processes, a strong depletion of the species makes the vibration temperature drop below the translational temperature, and this source term becomes positive. After that, the coupling effects of excitation and dissociation make the VT source term increase first then decrease to zero.

The DR and preferential DR energy source terms of the three molecular species are all negative during the relaxation, which means that the dissociation is dominant of the DR processes. After the onset of dissociation, the intensity of these processes increases as VT excitation pumps energy into higher vibrational levels. Then, as dissociation processes outweigh vibrational excitation, the strong depletion of the species consequently slows down dissociation. Thus, the DR energy source terms firstly reduce to the negative minima and raise back to zero when the reactions get to equilibrium. It is interesting to note that NO's preferential DR energy source term is nearly two orders of magnitude smaller than the non-preferential one and has the same order as the VT one, which demonstrates that DR for NO is close to a non-preferential character, while on the contrary, DR for the other two molecular species have strong preferential characters.

The Zeldovich reactions lead to a more complicated change in vibration energy and temperature. Analysis of the ZE energy source terms of N_2 shows that the reaction $N_2(v) + O \rightleftharpoons NO(w) + N$ consumes N_2 and creates NO at all times. Although Bose's rates produce less NO than Esposito's, the former absorb more N_2 vibrational energy than the latter. Besides, the solutions by Bose's rates show that the exchange reaction makes a negative contribution to N_2's vibration temperature, while the contribution predicted by Esposito's rates alternately decreases and increases the vibration temperature of N_2. However, these source terms are much smaller than either the VT and DR ones, so it is hard to observe their influence on the vibrational temperature. The ZE energy source terms of O_2 indicates that the formation of N observably initializes the reaction $O_2(v) + N \rightleftharpoons NO(w) + O$ at about 3×10^{-6} m which consumes O_2 and creates NO. Once NO is formed in sufficient amount, the reverse reaction takes over and leads to a production of O_2. Therefore, ZE energy source turns positive at about 10^{-4} m. This process slightly increases the vibration temperature of O_2 and slows down the consumption of O_2 by dissociation, as observed between 3×10^{-4} m to 5×10^{-4} m in Figure 1. Here, Bose's rates also present larger consumption or generation of energy to the O_2 vibrational mode. It is interesting to note from the preferential energy source terms that, this reaction by Bose's rates performs first negative then positive contribution to the vibration temperature of O_2, while it always increases the temperature by Esposito's rates. Finally, the joint effect of the two ZE exchange reactions gives a net increment to NO, but produces a non-monotonic change to the vibrational temperature.

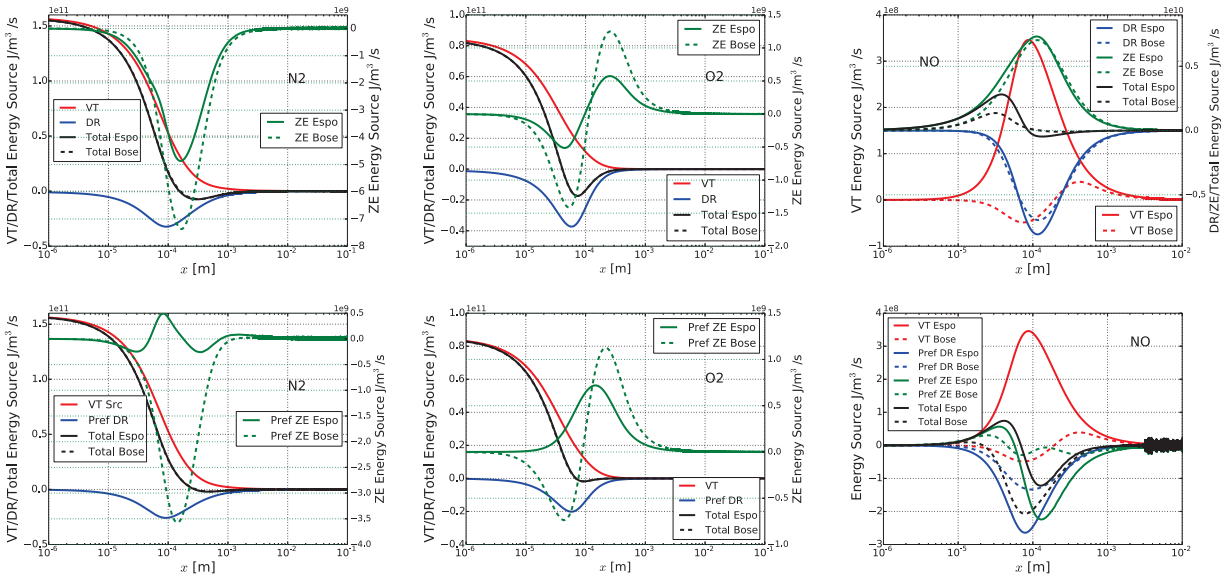

Figure 2. Profiles of vibrational energy source terms

A detailed investigation shows that Bose's rates to form high-lying levels of NO are significantly larger than Esposito's. This explains the vibrational temperature overshoot predicted with this model. On the other hand, Esposito's rates are larger for the formation of NO in intermediate-lying states. This leads to a larger production of NO. Note, however, that the original work [16, 17], only reported calculated rates for low and intermediate vibrational levels. Data for high-lying vibrational levels are obtained by extrapolation [8].

The rebuild intensity (red line) is compared to the measured intensity (black line) in Figure 3. The calculated spectra are obtained based on the results applied Esposito's rates. It is also worth to mentioned that the experimental one includes the radiative signature from all chemical species in air plasma. We also plot the radiation of N_2 system (blue dash line). In the range 200-300 nm the spectrum is dominated by NO systems with the small contribution of O_2 Shcumman-Runge, the agreement is pretty good, which could be recognized as valuable assessment of the data implemented for nonequilibrium NO modelling. However, the graph exhibits large discrepancy in the range above 300 nm, which is emitted by N_2. The first reason is that in the present calculation focused on NO, we neglected the N_2^+, although the First Negative system is important in our conditions. The other reason could be attributed to an overestimation of N_2 properties (or density, or temperature), which might be due to that the kinetic ionization mechanism is insufficient.

CONCLUSIONS

The vibration-specific State-to-State approach is employed to described vibrational relaxation and reactive processes in shock-heated air gas mixture consisting of the five chemical species N_2, O_2, NO, N and O. Vibrational state-specific description is adopted for molecules. There categories of physico-chemical processes are considered, including the vibration-translation energy exchange, dissociation-recombination and Zeldovich exchange reactions for NO formation. The detailed reaction rates are obtained from the FHO models or QCT calculations on *ab inito* potential energy surfaces. The classical models of Landau-Teller relaxation or Parks two temperature model are implemented in a state-specific way, where none of the above is available. The vibration-chemical kinetics in the relaxation region behind a shock wave with u = 8.06 km/s are discussed in detail. Radiative signatures of N_2, O_2 and NO are then determined and compared to experimental measurements. Results indicate the validity of the current model for NO formation.

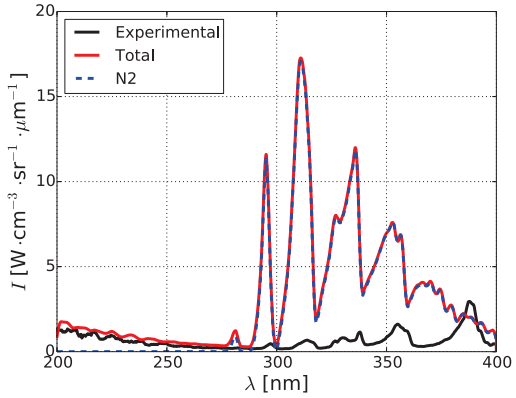

Figure 3. Profiles of spectral intensity of radiation from N_2, O_2 and NO

ACKNOWLEDGMENTS

This work has been partially supported by the UC3M CONEX-Marie Curie fellowship. Dr. Domenico Bruno and Dr. Wei Su would also like to acknowledge support from Italian project PON "Apulia Space" (03PE-00067-6).

REFERENCES

[1] C. Park, *Nonequilibrium Hypersonic Aerothermodynamics*, 1st ed. (Wiley-Interscience, New York, 1990).
[2] M. Capitelli, I. Armenise, E. Bisceglie, D. Bruno, R. Celiberto, G. Colonna, G. D'Ammando, O. De Pascale, F. Esposito, C. Gorse, V. Laporta, and A. Laricchiuta, Plasma Chem. Plasma Process. **32**, 427–450 (2012).
[3] A. Guy, A. Bourdon, and M.-Y. Perrin, Phys. Plasma **22**, 043507: 1–16 (2015).
[4] A. Munafo, Y. Liu, and M. Panesi, Phys. fluid. **27**, 127101: 1–22 (2015).
[5] D. A. Andrienko and I. D. Boyd, J. Chem. Phys. **144**, 104301: 1–19 (2016).
[6] M. Perrin, P. Riviere, and A. Soufiani, "Radiation database for Earth and Mars entry," Tech. Rep. (Centre National de la Recherche Scientifique, Chatenay-Malabry, France, 2008).
[7] A. Dikalyuk, P. Kozlov, Y. Romanenko, O. Shatalov, and S. Surzhikov, "Nonequilibrium Spectral Radiation Behind the Shock Waves in Martian and Earth Atmospheres," in *44th AIAA Thermophysics Conference* (San Diego, USA, 2013), pp. 1–27.
[8] B. Lopez, "Non-Boltzmann Analysis of Hypersonic Air Re-Entry Flows," in *11th AIAA/ASME Joint Thermoophysics and Heat Transfer Conference* (Atlanta, USA, 2014), pp. 16–20.
[9] K. Radhakrishnan and A. Hindmarsh, "Description and Use of LSODE, the Livermore Solver for Ordinary Differential Equations," Tech. Rep. (Lawrence Livermore National Laboratory, Livermore, CA, USA, 1993).
[10] R. C. Millikan and D. R. White, J. Chem. Phys. **39**, 3209–3213 (1963).
[11] M. Lino da Silva, STELLAR Database, http://esther.ist.utl.pt/pages/stellar.html, .
[12] I. V. Adamovich, S. O. Macheret, J. W. Rich, C. E. Treanor, and A. A. Fridman, in *Molecular Physics and Hypersonic Flows SE - 5*, NATO ASI Series, Vol. 482, edited by M. Capitelli (Springer Netherlands, 1996), pp. 85–104.
[13] M. Lino da Silva, B. Lopez, V. Guerra, and J. Loureiro, "A Multiquantum State-To-State Model For The Fundamental States Of Air And Application To The Modeling Of High-Speed Shocked Flows," in *5th Int. Workshop on Radiation of High Temperature Gases in Atmospheric Entry, ESA SP-714* (Barcelona, Spain, 2012).
[14] F. Esposito, I. Armenise, and M. Capitelli, Chem. Phys. **331**, 1–8 (2006).
[15] F. Esposito, I. Armenise, G. Capitta, and M. Capitelli, Chem. Phys. **351**, 91–98 (2008).
[16] D. Bose and G. V. Candler, J. Chem. Phys. **104**, 2825–2833 (1996).
[17] D. Bose and G. V. Candler, J. Chem. Phys. **107**, 6136–6145 (1997).
[18] F. Esposito, Submitted to J. Chem. Phys.